N86-17854

I-V-T ANALYSIS OF RADIATION DAMAGE IN HIGH EFFICIENCY Si SOLAR CELLS*

S. Banerjee, W. A. Anderson, and B. B. Rao
State University of New York at Buffalo
Buffalo, New York

High efficiency surface passivated N^+-P junction solar cells show deterioration in photovoltaic performance when subjected to 1 MeV electron irradiation. This change could be attributed to an increase in the dark saturation current after irradiation. A detailed analysis of the excess current using a thermal spectroscopic method reveals that the recombination mechanisms responsible for this effect can be identified as bulk recombination and space charge recombination through shallow traps. The former of these two mechanisms has a more severe effect and should be taken into account in the design.

INTRODUCTION

High efficiency silicon solar cells are widely used for space applications. Presently, silicon solar cells with efficiency $\sim$ 16% can be obtained routinely and finely tuned designs can yield even higher efficiencies (ref. 1,2). From time to time, various studies, both in-flight and on ground, are conducted to evaluate the stability of solar cells in a space environment. As a result of extensive research it is now understood that deterioration in photovoltaic performance is caused by a drastic increase in dark saturation current (ref. 3,4) which is evident from the following relationship,

$$V_{oc} = \frac{nkT}{q} \left[\ell n \frac{J_{sc}}{J_o}\right] \qquad (1)$$

where V_{oc} is the open circuit voltage, J_{sc} is the short circuit current density, J_o is the dark saturation current density, n is the diode ideality factor of the solar cell, and other symbols have their usual meanings. Following this lead, much research is being addressed towards understanding the mechanisms causing enhancement in J_o values in crystalline silicon solar cells (ref. 3).

It is well accepted that the current-voltage characteristics of a solar cell can be in general expressed as a double exponential behavior given by the simple relationship (ref. 3)

$$J = J_{DO} \left[\exp \frac{qV}{n_1 kT} - 1\right] + J_{RO} \left[\exp \frac{qV}{n_2 kT} - 1\right] \qquad (2)$$

where symbols have their usual meanings. The first term on the right is the diffusion current according to the theory developed by Shockley (ref. 5) and the second term on the right is the space charge recombination current given by Sah, et. al. (ref. 6). Equation (2) can be easily modified to incorporate the effect of series resistance (R_s) and shunt reistance (R_{sh}) of the solar cell. Results from different experiments (ref. 4) on N^+/P-P (passivated n^+-p junction) silicon solar cells indicate that it is the first term in eq. (2) which is changed after the cells were subjected to 1 MeV e^- irradiations at room temperature.

To investigate this effect further, dark and illuminated current-voltage characteristics of the aforementioned solar cells were studied as a function of temperature from 100 °K - 375 °K for which a marked increase in dark current was observed after the cells were irradiated. Activation energy plots indicate that under-illumination, diffusion current is the dominant component over much of the temperature range whereas under dark there is an excess current component besides the diffusion current. A simple analysis described elsewhere (ref. 7) was performed to extract this excess current component and the results will be discussed herein.

EXPERIMENTAL CONSIDERATIONS

Device Structure

Devices studied here have been supplied by Dr. Mark Spitzer of Spire Corp., Boston, and are fabricated on 0.3 Ω-cm boron doped silicon obtained from Wacker Chemtronics (standard WASO-grade). An n^+-p junction has been formed by 5 keV $^{31}P^+$ ion-implantation with an average dose of $\sim 2.5 \times 10^{15}$ ions/cm^2 resulting in a junction depth $\lesssim 0.5$ μm and emitter surface concentration $\sim 10^{20}$ cm^{-3}. The entire processing sequence and a schematic of the finished device are shown in reference 8.

Measurement Techniques

Solar cells were initially evaluated for their photovoltaic performance by measuring V_{oc}, J_{sc}, fill-factor (FF) and efficiency (η) at AM1 and AM0 intensity. However, only AM0 intensity parameters have been monitored after successive irradiation steps. Other measurements that were used to assess the cells include spectral response and diffusion length following the method developed by Stokes, et. al. (ref. 9).

Current-voltage characteristics have been measured in dark and under illumination as a function of temperature from 100 °K - 375 °K. Shunt resistance (R_{sh}) has been obtained from the slope of V_{oc}-I_{sc} measurements with very low illumination (ref. 10) performed at different temperatures in the aforementioned range. The series resistance R_s values at different temperatures have been obtained from the dark J-V characteristics using conventional techniques. The results obtained were quite consistent for different cells.

Irradiation Technique

After an initial assessment of the devices, some were subjected to 1 MeV e^- irradiation using a Van de Graff type electron accelerator. Devices were placed on a water-cooled sample holder to avoid any heating during irradiation. The electron beam was rastered across the entire sample holder in order to ensure a uniform irradiation. Irradiation dose was varied from 1×10^{14} e^-/cm^2 - 1×10^{16} e^-/cm^2 increased by an order each time. All the devices were tested for their photovoltaic performance after successive irradiations.

DATA ANALYSIS

The photovoltaic measurements are used as a performance check at different stages of irradiation. The major emphasis is on the current-voltage characteristics in dark and under illumination for which a simple method of analysis will be described. From the dark and illuminated current-voltage characteristics, dark and light ideality factors (n_d and n_ℓ, respectively) and saturation current densities (J_{do} and $J_{\ell o}$, respectively) have been extracted using the straight line portions of the curves at a bias voltage approximately equal to the V_{oc} at each temperature. Using J_{do} and $J_{\ell o}$ values at different temperatures, Arrhenius plots were made to obtain the activation energy.

The analysis of experimental current-voltage behavior is based on a model which can be expressed as (ref. 7),

$$J_{Total} = J_{od} \left[\exp \frac{qV_d}{n_D kT} - 1\right] + J_{Excess} \qquad (3)$$

where J_{Total} is the total measured diode current density, J_{od} is the saturation current density for the diffusion component, V_d is the diode bias voltage, n_D is the ideality factor for diffusion mechanism, and J_{Excess} is the excess current component responsibe for enhancement of J_{Total} from its ideal value. The only assumption made here, to be justified later, is that ideally the total current should have only a diffusion component. Furthermore, J_{Excess} is not given any functional form as in some earlier works (refs. 3,11). Voltage and temperature dependences of J_{Excess} have been studied to obtain the nature of J_{Excess}.

To extract J_{Excess} from the experimental data eq. (3) is modified to incorporate the effect of R_s and R_{sh}. Thus,

$$I_{Total} = I_{od} \left[\exp \frac{q(V-I_{Total}\,R_s)}{n_D kT} - 1\right] + I_{Excess} + \frac{V-I_{Total}\,R_s}{R_{sh}} \qquad (4)$$

where V is the terminal voltage and

$$V = V_d + I_{Total}\,R_s \qquad (5)$$

To calculate I_{Excess} from the experimental data, I_{od} and n_D in eq. (4) were replaced by $J_{\ell o}$ x A and n_ℓ, respectively, where A is the area of the cell. The reason for this change will become aparent in the next section. Finally, J_{Excess} is calculated as I_{Excess}/A. The J_{Excess} thus obtained is plotted as a function of voltage with temperature as a parameter. The results of this analysis will be discussed in the next section.

RESULTS AND DISCUSSION

Typical current-voltage characteristics (in dark) for N^+-P/P silicon solar cells before and after e^- irradiation are shown in Figures 1 and 2, respectively. It is clear from the graphs that the total current density is higher in the latter case. Also, the shape of the curve for low temperatures and intermediate voltage range is different in the two cases due to the fact that in this particular voltage regime, shunt current given by the last term in eq. (4) is the dominant component of the total current especially at the lower temperatures. Therefore, the remaining two terms are masked by this effect. However, after the cells were irradiated by 1 MeV e^- to a dose of 1×10^{16} e^-/cm^2, this particular component is not affected as much as the other two terms i.e., the diffusion and the excess current, hence the slope of the ℓn J vs V is slightly higher than those in Figure 1 for the same voltage regime. As the temperature is raised, the first two terms in eq. (4) become larger than the shunt resistance current and the flat region in the ℓn J vs V curves disappear. The straight line region of these curves near the V_{oc} values at each temperature is used to extract the J_{do} and n_d values. The n_d values obtained vary typically between 1.27 - 1.43 and 1.21 - 2.08 before and after irradiation, respectively, indicating the presence of a mechanism(s) other than diffusion. The J_{do} values obtained from the dark J-V characteristics before and after irradiation show a two orders difference due to a change expected in the diffusion length values. Independent measurements of diffusion length and spectral response support this result. Using the J_{do} values, Arrhenius plots were drawn as shown in Figures 3 and 4 from which activation energies* were typically 0.95 eV and 0.85 eV, respectively. This further suggests that there is a deviation from a purely diffusion mechanism, where activation energy should equal 1.12 eV, which is larger after irradiation.

A similar analysis for the illuminated current-voltage (J_{sc} - V_{oc}) characteristics with a typical plot shown in Figure 5, gives n_ℓ values of 1.04 - 1.10 and 1.04 - 1.12 before and after irradiation, respectively. However a two orders of magnitude difference in $J_{\ell o}$ values were also observed in this case. Following the same arguments as in the case of J_{do}, it is suggested that a bulk recombination current component is responsible for the enhancement of J_{do} and $J_{\ell o}$ values after e^- irradiation. Arrhenius plots using $J_{\ell o}$ values shown in Figures 3 and 4 yield activation energies of 1.18 eV and 1.14 eV before and after irradiation, respectively, suggesting that a diffusion current is the dominant component. It should be noticed that in the latter case this diffusion current is a combination of ideal diode current and the bulk recombination current which has a same temperature and bandgap energy (E_g) dependence as the ideal diode current (ref. 3). Furthermore, it can be inferred that under illumination these solar cells show a near ideal diode behavior due to the fact that photo-carriers fill the traps responsible for space charge recombination mechanism(s), however, it is not possible to identify these mechanisms at this stage of analysis.

* Values obtained are not corrected for the temperature dependence of bandgap energy (E_g).

Figures 6 and 7 show typical excess-current ℓn J_e vs V characteristics before and after irradiation, respectively, where excess current components were obtained from eq. (4), and represent recombination current components. From Figure 6 it is obvious that there are two regions with different slopes for each temperature whereas in the case of the cells after irradiation (Figure 7) there are two different temperature regions for which the slopes are entirely different. In the former case the ideality factors in the low slope region are calculated to be closer to 2 while the ideality factors are calculated to be closer to 1 for the higher slope region. Furthermore, the ideality factors increase with decrease in temperature. The J_{eo} (excess saturation current density) obtained for the different regions were used to make Arrhenius plots shown in Figure 8. The lower slope region gives an activation energy of 0.565 eV indicating a recombination through deep traps (ref. 6), whereas the upper slope region yields an activation energy of 0.763 eV indicating a recombination mechanism through shallow traps in the space charge region which corresponds to a trap level approximately equal to 0.706 eV (ref. 3) after correcting for the temperature effect of E_g and the energy difference between $E_g/2$ and intrinsic level E_i. This behavior differs from what has been observed in the previous work (ref. 3) using diffused junctions and can be attributed to incomplete annealing of ion-implantation damage.

A typical Arrhenius plot for the cells after irradiation is also shown in Figure 8. Unlike in the previous case, there are two distinct slopes in different temperature regions. In the higher temperature region, 250 °K - 375 °K, an activation energy of 0.763 eV has been obtained, following the previous procedure, which correspond to a trap level of 0.706 eV. A very low activation energy of 0.124 eV is obtained between 110 - 280 °K. The ideality factors obtained from the ℓn J_e vs V plots in this case is closer to 1 at higher temperatures and increases to more than 2 as the temperature is decreased. Variation of ideality factor in N^+-P junction solar cells can be explained by a distribution of traps in the space charge region rather than a single trap level (ref. 11,6). The reoccurrance of the 0.706 eV level as the dominant shallow trap further makes one believe that this is inherent to the implantation. It is possible that there are other shallow traps developed after irradiation, however, if the trap-levels are very closely spaced, it is difficult to identify each of those using such a simple approach.

CONCLUSION

A detailed analysis of current-voltage characteristics of N^+-P/P solar cells indicate that there is a combination of different mechanisms which results in an enhancement in the dark current and in turn deteriorates the photovoltaic performance of the solar cells after 1 MeV e^- irradiation. The increase in the dark current is due to three effects i.e., bulk recombination, space charge recombination by deep traps and space charge recombination through shallow traps. It is shown that the increase in bulk recombination current is about 2 - 3 orders of magnitude whereas space charge recombination current due to shallow traps increases only by an order or so and no space charge recombination through deep traps was observed after irradiation. Thus, in order to improve the radiation hardness of these devices, bulk properties should be preserved.

REFERENCES

1. Spitzer, M. B.; Keaveny, C. J.; Tobin, S. P.; and Milstein, J. E.; "Ion Implanted Silicon Solar Cells with 18% Conversion Efficiency," Proc. 17th Photovoltaic Specialists Conference, Kissimmee, Florida 398-402, 1984.

2. Green, M. A.; Blakers, A. W.; Jiqun, S.; Keller, E. M.; Wenham, S. R.; Godfrey, R. B.; Szpitalak, T.; and Willison, M. R.; "Towards A 20% Efficient Silicon Solar Cell," Proc. 17th Photovoltaic Specialists Conference, Kissimmee, Florida, 386-389, 1984.

3. Wolf, M.; Noel, G. T.; and Stirn, R. J.; "Investigation of the Double Exponential in the Current-Voltage Characteristics of Silicon Solar Cells," IEEE Trans. Electron Dev., ED-24, #4, 419-428, 1977.

4. Anderson, W. A.; Solaun, S.; Rao, B. B.; and Banerjee, S.; "Influence of Design Variables on Radiation Hardness of MINP Solar Cells," Space Photovoltaic Research and Technology Conf., Cleveland, Ohio, 1985.

5. Shockley, W.; "The Theory of P-N Junctions in Semiconductors and P-N Junction Transistors," Bell Syst. Tech. J., 28, 435-489, 1949.

6. Sah, C. T.; Noyce, R. N.; and Shockley, W.; "Carrier Generation and Recombination in P-N Junctions and P-N Junction Characteristics," Proc. IRE, 45, 1228-1243, 1957.

7. Rao, B. B.; Banerjee, S.; Anderson, W. A.; and Han, M. K.; "Excess Currents in MINP Type Solar Cells," IEEE Trans. Electron Dev., ED-32, #4, 817-821, 1985.

8. Spitzer, M. B.; Tobin, S. B.; and Keavney, C. J.; "High Efficiency Ion-Implanted Solar Cells," IEEE Trans. Electron Dev., ED-31, #5, 546-550, 1984.

9. Stokes, E. D.; and Chu, T. L.; "Diffusion Lengths in Solar Cells from Short Circuit Current Measurement," Appl. Phys. Lett., 30, #8, 425-426, 1977.

10. Chan, D. S. H.; and Phang, J. C. H.; "A Method for the Direct Measurement of Solar Cell Shunt Resistance," IEEE Trans. Electron Dev., ED-31, #3, 381-383, 1984.

11. Stirn, R. J.; "Junction Characteristics of Silicon Solar Cells," Proc. 9th Photovoltaic Specialists Conference, Silver Springs, Maryland, 72-82, 1972.

* The work described in this paper was performed in part under the sponsorship and technical direction of International Telecommunications Satellite Organization (INTELSAT). Any views expressed are not necessarily those of INTELSAT.

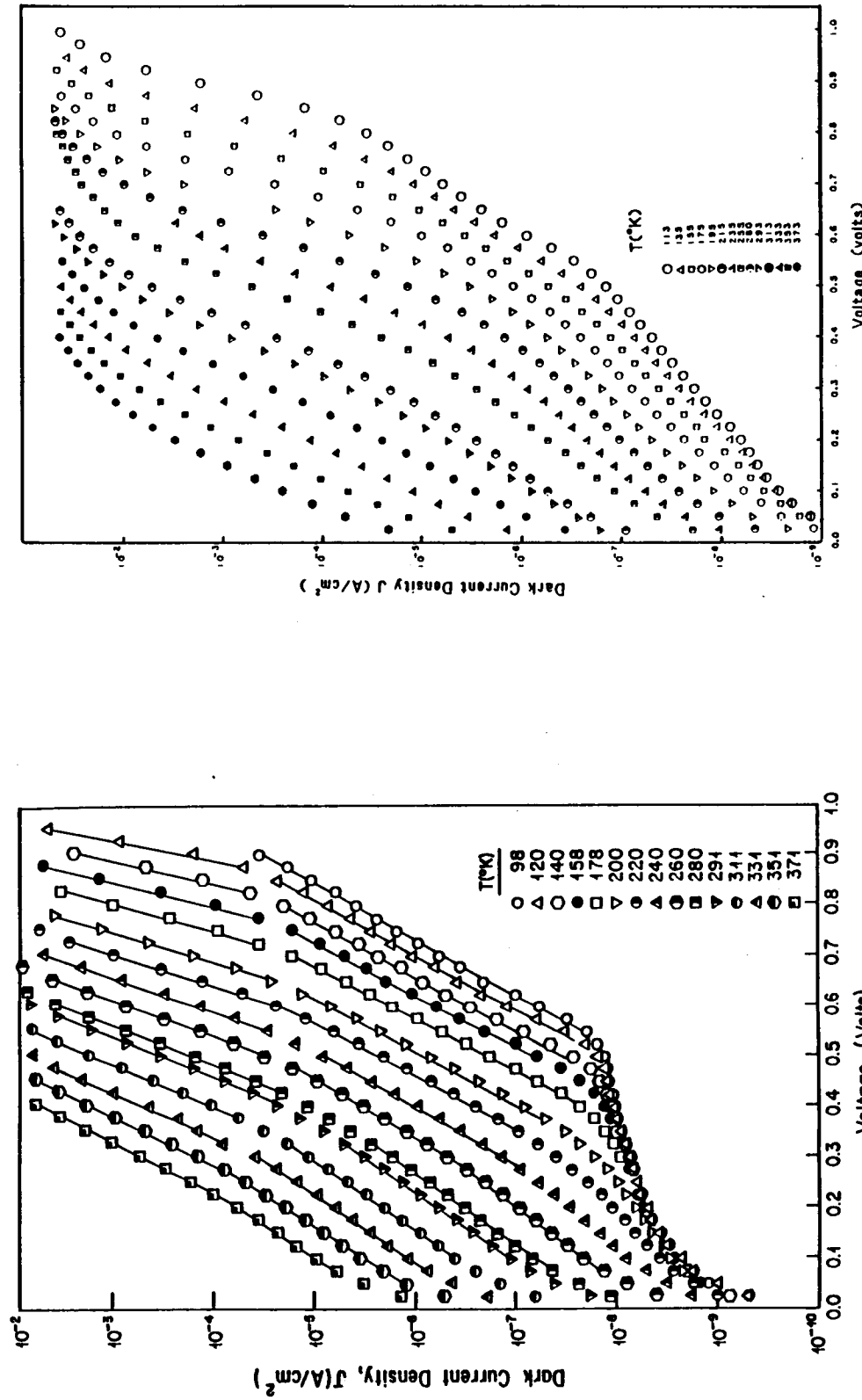

Figure 1. Typical Dark J-V curves before irradiation.

Figure 2. Typical Dark J-V curves after irradiation

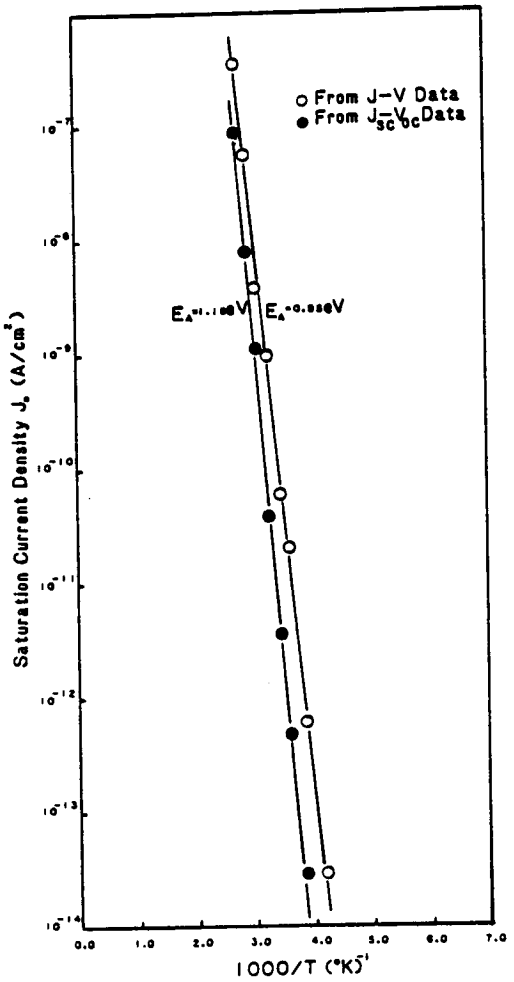

Figure 3. Arrhenius plots before irradiation

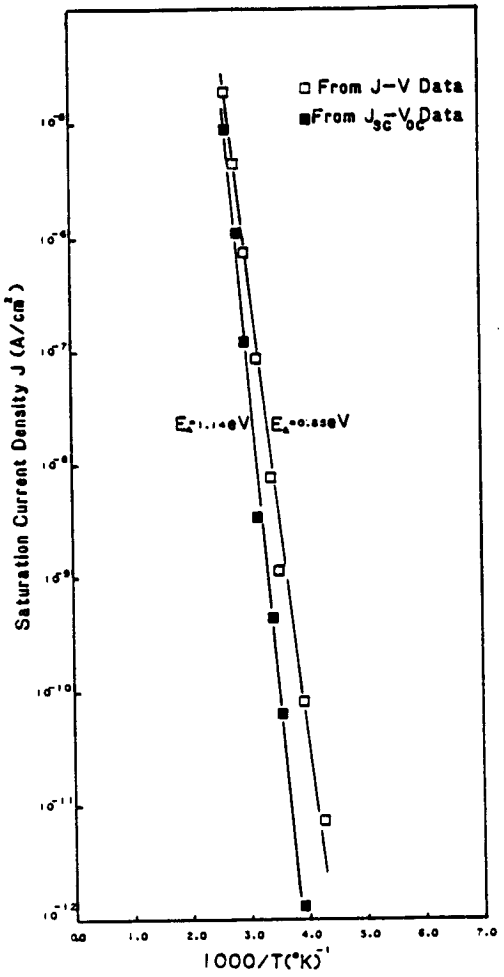

Figure 4. Arrhenius plots after irradiation

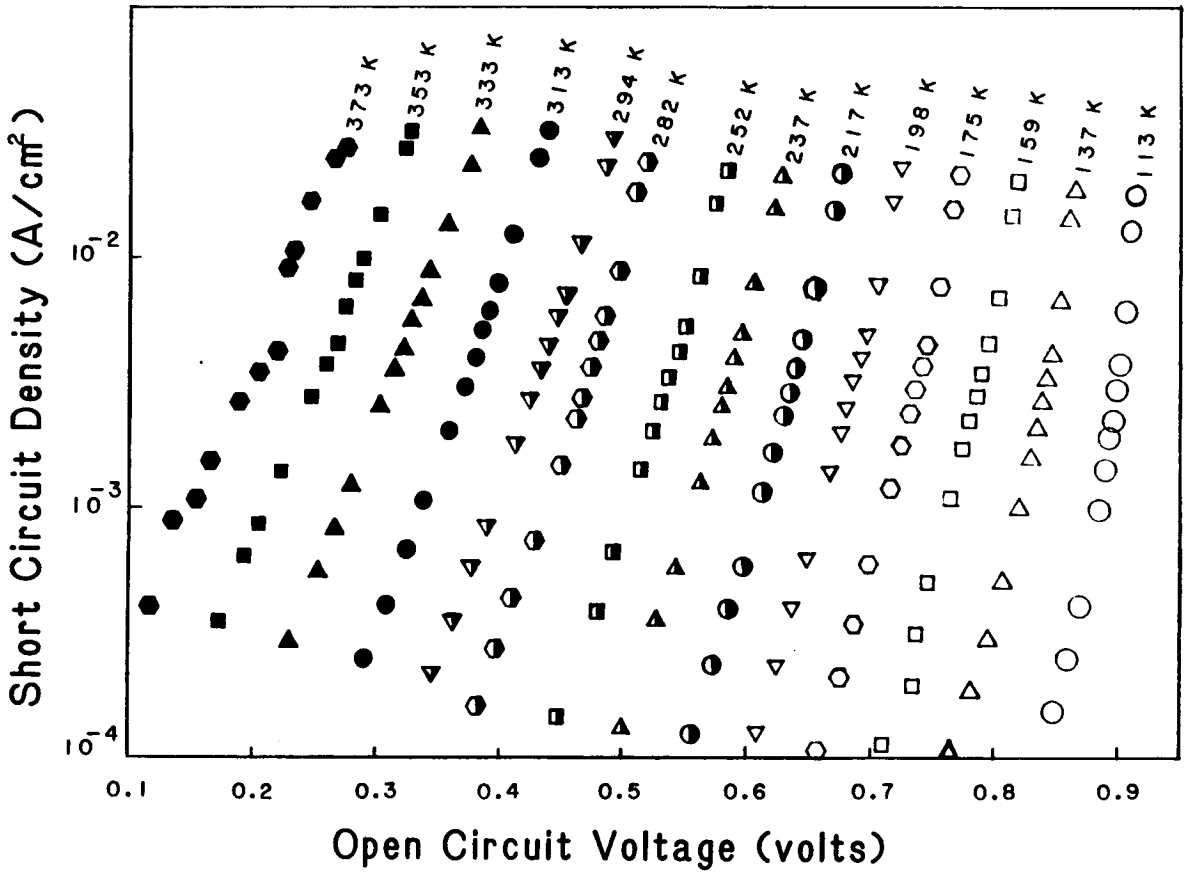

Figure 5. Typical Illuminated Current-Voltage (J_{sc}-V_{oc}) Curves

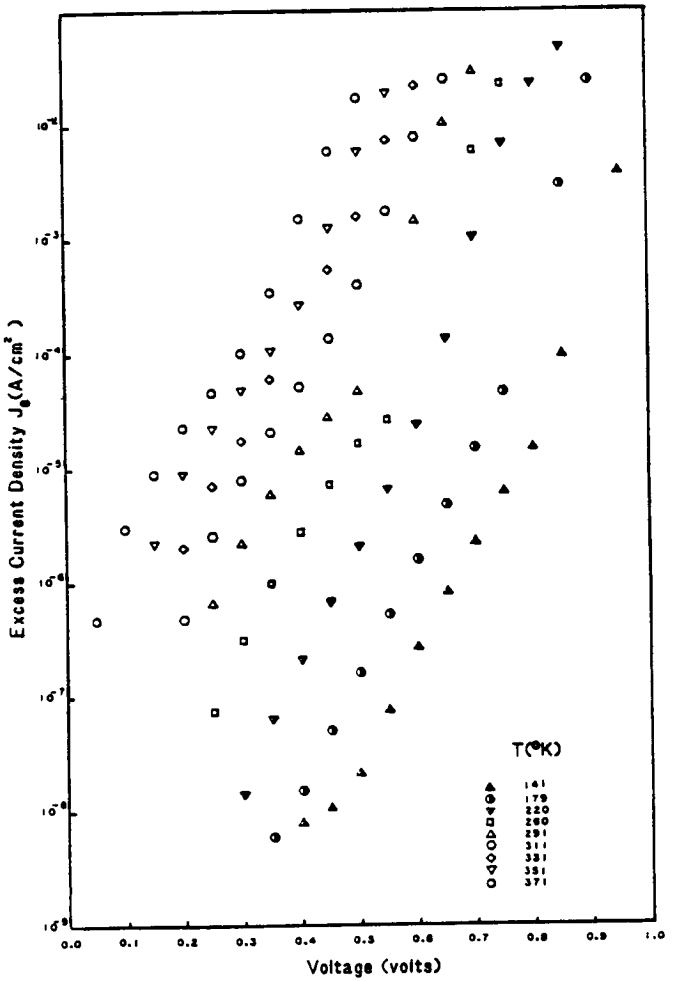

Figure 6. Typical Excess-Current J_e-V Curves Before Irradiation

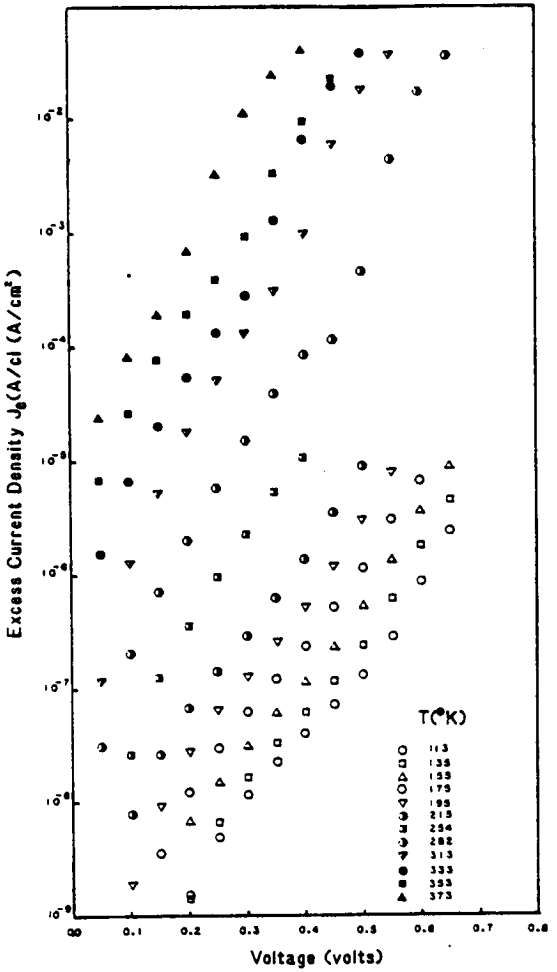

Figure 7. Typical Excess-Current J_e-V Curves After Irradiation

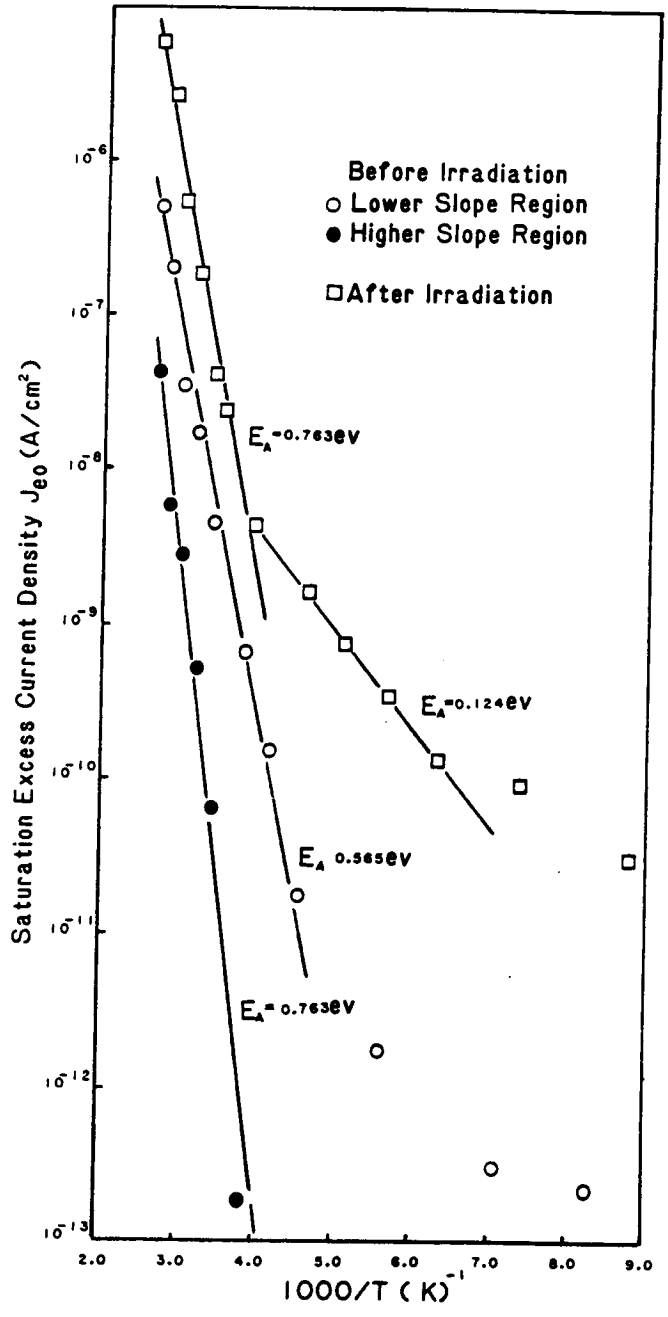

Figure 8. Arrhenius plots for saturation value of Excess-Current Density (J_{eo}).